

Direct CO₂ Activation and Conversion to Ethanol via Reactive Oxygen Species

Alina Meindl, *^[a] and Mathias O. Senge^[b, c]

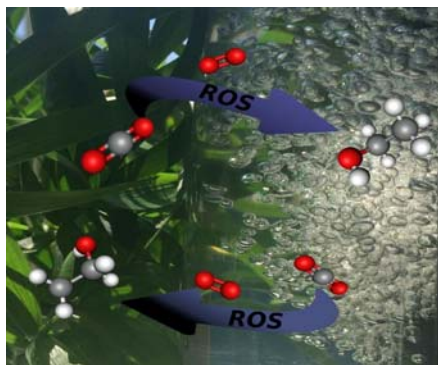
[a] Dr. A. Meindl
Department of Green Engineering and Circular Design
Salzburg University of Applied Sciences
Markt 136a, 5431 Kuchl, Austria
E-mail: alina.meindl@fh-salzburg.ac.at

[b] Prof. M.O. Senge
Institute for Advanced Study (TUM-IAS), Focus Group – Molecular and Interfacial Engineering of Organic Nanosystems
Technical University of Munich
Lichtenbergstrasse 2a, D-85748 Garching, Germany

[c] Prof. M.O. Senge
School of Chemistry
Trinity College Dublin, The University of Dublin
Trinity Biomedical Sciences Institute, 152–160 Pearse Street, Dublin 2, Ireland

Supporting information for this article is given via a link at the end of the document.

Abstract: The growing demand for energy and the excessive use of fossil fuels represents one of the main challenges for humanity. Storing solar energy in the form of chemical bonds to generate solar fuels or value-added chemicals without creating additional environmental burdens is a key requirement for a sustainable future. Here we use biomimetic artificial photosynthesis and present a dPCN-224(H) MOF-based photocatalytic system, which uses reactive oxygen species (ROS) to activate and convert CO₂ to ethanol under atmospheric conditions, at room temperature and in 2–5 h reaction time without the use of sacrificial donors. The system provides a CO₂-to-ethanol conversion efficiency (CTE) of 92%, while attaining a selectivity for EtOH formation. Furthermore, this method also allows the conversion of CO₂ through direct air capture (DAC), making it an incredibly fast and versatile method for both dissolved and gaseous CO₂.



Introduction. In 2019 humankind used 4.4 billion tons of fossil fuels. At the same time global warming increased by an average of 1.2 °C compared to pre-industrial level, making 2020 the warmest year on record.^[1–4] The situation is unsustainable and critical. This has also been pointed out very starkly by UN Secretary-General António Guterres at the COP26: “The six years since the Paris Climate Agreement have been the six hottest years on record. Our addiction to fossil fuels is pushing humanity to the brink.” CO₂ is one of the main protagonists in the unfolding climate and energy drama and, thus, conversion of CO₂ into renewable and carbon-zero fuels and chemical building blocks increasingly attracts the attention of the research community and the focus has shifted towards the exploration of sustainable energy to target these issues.^[5–8] Using greenhouse gases such as CO₂ as starting

materials and converting them into valuable chemicals and fuels is among the requirements of a sustainable chemical industry.^[9,10] Natural bio-derived fuels and chemicals often compete with food production, require prime agricultural land, resulting in ecological disruption. Artificial photosynthesis - the sunlight-driven production of fuels using synthetic catalysts - can, however, use resources that would otherwise be considered waste or even greenhouse gases.^[11,12] This field has advanced significantly since the discovery of photoelectrochemical water splitting using TiO₂ and platinum.^[13] These achievements range from understanding the fundamentals of the biological processes and metalloenzymes, to the development of inorganic catalysts and electro- and photocatalytic systems for solar-fuel generation.^[14–17] Furthermore, thermal hydrogenation or the direct use of CO₂ in chemical syntheses are promising applications.^[18,19] Usually, reduction products from two-electron transfer processes (H₂, CO and formate) are formed; however, recently also multi-electron products such as methane or methanol have been reported.^[20–22] Fundamental challenges remain and need to be overcome for efficient photocatalysis of CO₂ to become a viable and practical method. A major problem is the activation of CO₂, which has proven to be extremely difficult.^[23] Additionally, the use of sacrificial donors is often necessary.^[24–26] These components are often considered the ‘necessary evil’ when it comes to artificial photosynthesis and are required to push the reactions from low energy substrates to high value products. Such sacrificial donors include aliphatic and aromatic amines, benzyl-dihydropyridinamide (BNAH), dimethylphenylbenzimidazole (BIH), ascorbic acid, oxalate and thiols, among others.^[27] These compounds - often used in high molar ratios of 1000:1 compared to the photocatalyst - must be taken into consideration when evaluating an artificial photochemical system for its ‘green potential’.^[28] Further challenges are high overpotentials and slow reaction rates of the catalysts; controlling the reaction pathway to generate a carbon-based product selectively, low-concentration CO₂ sources such as flue gas (10–25%) or air (~400 ppm); alignment of semiconducting materials with panchromatic visible light absorption, the stability and the long-term durability of catalysts, as well as the use of expensive rare metals.^[10, 29–34] Natural processes often provide superior examples while challenging researchers to mimic their function with related compounds.

Organic multicomponent systems are a logical next step for electronic applications due to ample natural examples, such as photosystems and ion conducting channels, etc.^[35]

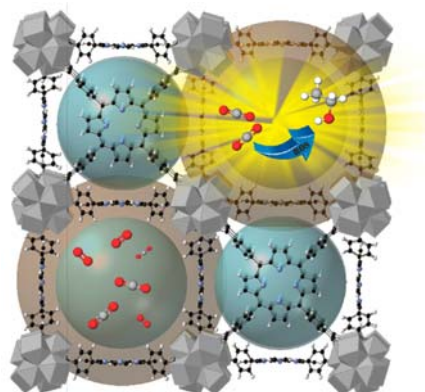


Figure 1. CO₂ to EtOH conversion via ROS.

While natural systems are suitable as models, they are far too unstable for direct translation to industrial photonics. Hence, multicomponent structures are necessary to accurately imitate them.^[36] Consequently, large stable heteroaromatic systems such as porphyrins with tunable electronic properties are interesting materials for these applications. Porphyrins can readily generate reactive oxygen species (ROS), such as singlet oxygen or superoxide ions, which are known to play major roles in different applications due to their fast generation and reactivity.^[37-41] In this paper, we report a method for CO₂ activation via the photochemical reaction with ROS, utilizing a well-known metal-organic framework dPCN-224(H) (MOF) which incorporates the free base 5,10,15,20-tetrakis(4-carboxyphenyl)porphyrin as photosensitizer (Figure 1). Incorporation of the porphyrin into a MOF results in a stable heterogeneous photocatalyst. The utilized photosensitizer converts CO₂ efficiently and rapidly (2-5 h) into ethanol with a conversion rate of 92%. The reaction proceeds under mild reaction conditions, namely under atmospheric conditions and at room temperature, while relying on a simple light emitting diode (LED) as light source, in contrast to commonly used high-power light sources.^[42] Flexibility in using gaseous or dissolved CO₂ can allow use of more efficient sources for direct capture.^[43]

Results and Discussion. Previously developed protocols were used to generate the photoactive material dPCN-224(H).^[44] Photosynthetic reactions were carried out in closed plastic containers (5 mL) with side illumination of a commercial LED lamp. 16 mg of photoactive material dPCN-224(H) were used per mL reaction media (H₂O) for all experiments performed. The progress of the photoreaction was monitored using infrared (IR) spectroscopy. Mid-IR spectra were recorded using a custom built multibounce attenuated total reflection (ATR). The setup has been incorporated into a Fourier transform IR (FT-IR) spectrometer and was reported before.^[45] Samples of the liquid headspace of the immobilized catalyst were taken and injecting it into the 20 μ L flowcell

utilizing a sequential injection analysis (SIA) system. For each measurement a total of 100 μ L sample was injected. Besides this, also the pH value, dissolved oxygen content (DO) and temperature were measured (see Table S1). The integral of the dominant CO-stretching band was used to determine the ethanol concentration in the reaction mixture. Therefore, a calibration curve ranging from 5 mM to 100 mM ethanol concentrations was generated (Figure S1). Furthermore, the limit of detection (LOD) was calculated according to Formula 1.^[46] With S_{blank} being the standard deviation of five consecutive measurements of the water-filled cell the LOD resulted in 0.05 mM ethanol.

$$LOD = \frac{3 * S_{blank}}{\text{slope of the calibration curve}} \quad (1)$$

The recorded IR spectra showed a rapid production of EtOH over 5 h indicated by the increase of the $\nu(\text{C-O})$ ^[47] band at 1044 cm^{-1} in Fig. 2a upon the exposure of dPCN-224(H) to simulated solar irradiation (white light, LED, 10 mW) in a CO₂-saturated aqueous solution (pH: 4.2; DO: 2.7 ppm; temp.: 22.6 °C) under atmospheric conditions (1 atm.). The increase of EtOH concentration was accompanied by CO₂ consumption proven by the decrease of the $\nu(\text{C=O})$ band of CO₂ at 2344 cm^{-1} , the respective spectral regions are shown in Figure 2a and 2b.^[47] Formation of ethanol was observed after a reaction time of 1 h (Figure 2c). Furthermore, the generation of ROS was confirmed using a standard ROS probe experiment (see Figure S2).^[48] The concentration of dissolved CO₂ was determined (Figure S3) and the photosensitizer was added to the reaction mixture.^[49] The CO₂ at the start amounted to 26.4 mmol/L, which decreased to 1.1 mmol/L over 5 h. At the same time 3 mmol/L EtOH were formed within the first hour, increasing to 12.2 mmol/L after 5 h reaction time (Figure 2a). This equals a CO₂-to-ethanol conversion efficiency (CTE) of 92%. All obtained ethanol concentrations were larger than the 0.05 mM LOD, making this the perfect method of choice in this investigation, as it enabled not only a quantitative evaluation but also a stoichiometric investigation of CO₂ activation and conversion. The reaction mixture after 5 h was compared to a 10 mM EtOH solution (Figure 2b) and the reaction progress was monitored (Figure 2c). Furthermore, reproducibility experiments were performed utilizing 16 mg photoactive material/mL reaction media for each run. The formation of EtOH in mmol/L during six different experiments is shown in Figure 2d. The average concentration of EtOH produced during these experiments amounts to 12.1 mM with a relative standard deviation of 4.7 %. All details are given in Table S1. Other high CO₂ conversion rates have been reported in literature. Reisner et al. for example achieved a production rate of $83.9 \pm 5.8\%$ for CO₂ conversion to HCOO⁻.^[33] Li et al. recorded a near 100% CO₂ conversion to formate,^[50] while Ye et al. reported a 80% CO₂ to CH₄ conversion rate.^[51] Li et al. published a CO₂ to methanol conversion of 1712.7 $\mu\text{mol/g}$,^[52] which is slightly higher than the 1220 $\mu\text{mol/g}$ conversion rate we achieved for ethanol. Zhang et al. synthesized metal-organic frameworks-derived

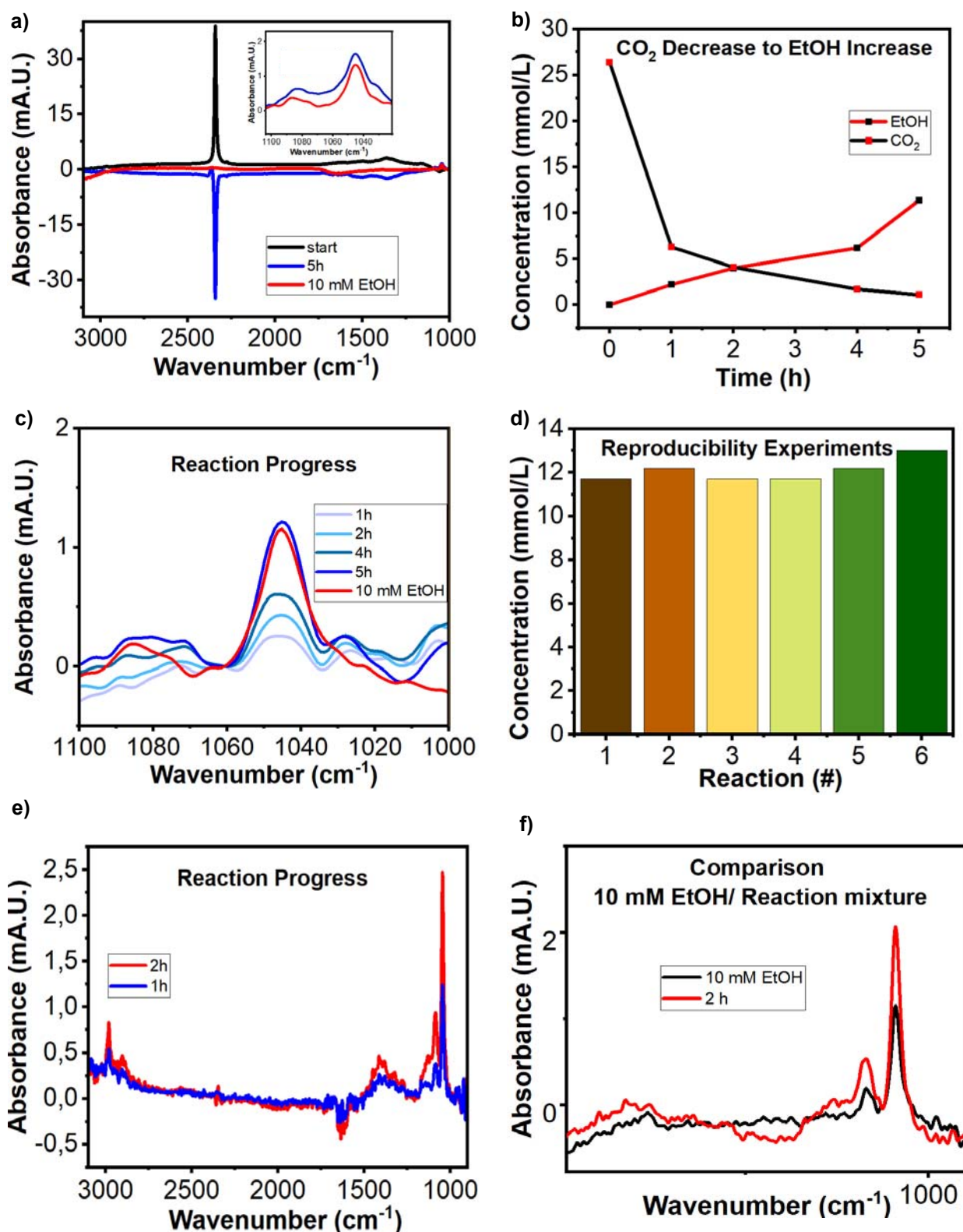


Figure 2. Re-

action progress. a) Reaction at room temperature with 16 mg photoactive material/mL reaction media at a starting CO₂ concentration of 26.4 mmol/L, b) Comparison of EtOH increase and CO₂ decrease, c) Reaction progress over 5 h and comparison to 10 mM EtOH, d) Reproducibility experiments: EtOH formation during six different experiments at room temperature with 16 mg photoactive material/mL reaction media. e) Reaction progress direct air capture experiments (DAC) after 1 h and 2 h at room temperature with 16 mg photoactive material/mL reaction media. f) Comparison of reaction outcome DAC to 10 mM EtOH reference.

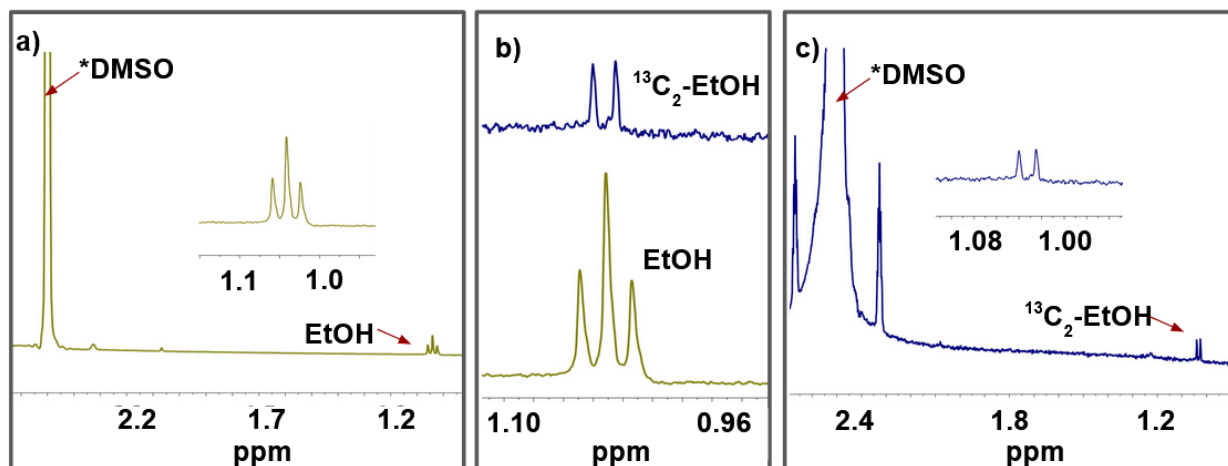


Figure 3. NMR Spectra. a) $^1\text{H-NMR}$ spectra (400 MHz, DMSO) of EtOH (green). b) Comparison $^1\text{H-NMR}$ spectra (400 MHz, DMSO) of EtOH (green) and $^{13}\text{C}_2$ -EtOH (blue). c) $^1\text{H-NMR}$ spectra (400 MHz, DMSO) of $^{13}\text{C}_2$ -EtOH (blue).

nanomaterials for ethanol production from CO_2 and achieved a high faradaic efficiency of 70.52%.^[53] Furthermore, Xie et al. reported a CO_2 to ethanol conversion with 98.35% selectivity.^[54] While some MOFs with incorporated porphyrins have been reported in literature as catalysts for CO_2 conversion, they either utilize metallized porphyrins where the metal core itself facilitates the catalytic reaction, use sacrificial agents or the porphyrin is simply employed as an organic linker for charge transfer.^[55-59] The novelty of our system lies in the use of metal-free porphyrins, which catalyze the reaction through ROS without the need of any sacrificial agents, in combination with very mild reaction conditions. To determine the potential species involved in the reaction, we performed the following exclusion experiments: No products were obtained either in the absence of light (pH: 4.1; DO: 2.3 ppm; temp.: 22.2 °C) or the photocatalyst (pH: 4.0; DO: 2.7 ppm; temp.: 22.3 °C) under the same conditions (Figure S4 and S5). These results rule out the possibilities of reduction/oxidation of impurities acting as sacrificial reagents.^[33] Furthermore, no products were detected during control experiments performed in aqueous solutions without CO_2 (pH: 5.9; DO: 4.4 ppm; temp.: 22.7 °C) or O_2 (purged with N_2 for 2h, pH: 4.2; DO: 0.1 ppm; temp.: 22.5 °C), respectively (Figure S6 and S7). These observations indicate that EtOH was produced via photochemical CO_2 conversion rather than decomposition of the photocatalyst and simultaneously highlights the catalytic activity of dPCN-224(H) for solar fuel production. To show that the photosensitizers, together with the resultant ROS, are the indispensable parts of the photocatalyst; a blank material was synthesized exchanging the photosensitizer with terephthalic acid. Again, no product formation was observed under the reaction conditions (pH: 4.0; DO: 2.7 ppm; temp.: 22.3 °C) (Figure S8). This further corroborates the involvement of ROS in the CO_2 conversion reaction and the absence of any decomposition products. The formation of ethanol was also confirmed by $^1\text{H-NMR}$ spectroscopy (Figure 3a). In addition, isotopic labelling experiments with $^{13}\text{CO}_2$ confirmed the formation of $^{13}\text{C}_2$ -EtOH by its characteristic $^1\text{H-}^{13}\text{C}$ splitting pattern of a doublet at 1.04 ppm compared to the usual triplet visible under atmospheric conditions (Figure 3b,c).^[60] While the exact reaction mechanism involved is still part of ongoing investigations, some reports suggest that superoxide ions can readily react and convert CO_2 .^[61,62]

Photochemical Reaction and Photosynthetic CO_2 Conversion via Direct Air Capture (DAC). The photoactive catalyst was also exposed to direct air capture conditions (DAC). In this process CO_2 is directly captured from ambient air without any additional saturation or addition of CO_2 . Under ambient conditions CO_2 is present in air at a relative low concentration of 400 ppm. The DAC technology has been extensively researched over the last decades as a promising method to remove CO_2 proactively from the atmosphere and store it permanently as a solid.^[63,64] In contrast to those previous studies, we decided to take this approach one step further, by not only removing the CO_2 from the air for storage but also utilizing it as a value-added starting material for photochemical reactions via ROS activation. In this experiment the dry catalyst was put on a frit and air was pumped through the photoactive material for 2 h at a rate of 2.3 m^3/h , allowing it to adsorb CO_2 from ambient air. The sensitizer was then added to distilled water. Again, as shown in Fig. 2e, rapid production of EtOH occurred upon the exposure of dPCN-224(H) to simulated solar irradiation (white light, LED, 10 mW) in aqueous solution (pH: 5.3; DO: 4.3 ppm; temp.: 22.8 °C) under atmospheric conditions (1 atm.). Already after 1 h reaction time the formation of ethanol could be observed. The concentration of ethanol produced amounted to 16.1 mmol/L after 2 h of reaction time (Figure 2f). This is a significantly higher concentration than in the experiments with dissolved CO_2 , which indicates the solubility of CO_2 in water to be the limiting factor in the previous reaction. No products were obtained either in the absence of light (pH: 5.4; DO: 4.4 ppm; temp.: 22.6 °C) or the photocatalyst (pH: 5.4; DO: 4.3 ppm; temp.: 22.7 °C) under the same conditions (Figure S9 and S10). Furthermore, no products were detected during control experiments in aqueous solutions with the blank material (pH: 5.3; DO: 4.2 ppm; temp.: 22.6 °C) (Figure S11). These experiments showcase the efficiency and flexibility of this method and the potential of combining DAC with dissolved CO_2 .

Conclusions. A new approach to activate and convert CO_2 in dissolved as well as gaseous form via ROS was established. The method proved to be highly efficient in converting CO_2 under atmospheric conditions and at room temperature within 5 h into ethanol. 12.2 mmol/L of ethanol were generated when using CO_2

saturated water which equals a CTE of 92 %. This performance is the result of the combined high selectivity and high activity of the free base catalyst without the need of sacrificial reagents. Furthermore, DAC measurements resulted in 16.1 mmol/L of EtOH, which demonstrated the possibility to convert both dissolved as well as gaseous CO₂ from the atmosphere. This showcases both the inherent flexibility of this method as well as its efficiency, which could be even further increased by increasing the CO₂ concentration. Future work will include the investigation into the exact reaction mechanism and the ROS species involved.

Acknowledgements

This work was prepared with the support of the Technical University of Munich – Institute for Advanced Study through a Hans Fischer Senior Fellowship and received funding from Science Foundation Ireland (IvP 13/IA/1894). We would like to acknowledge the help of Dr. Christopher J. Kingsbury for proof-reading the manuscript.

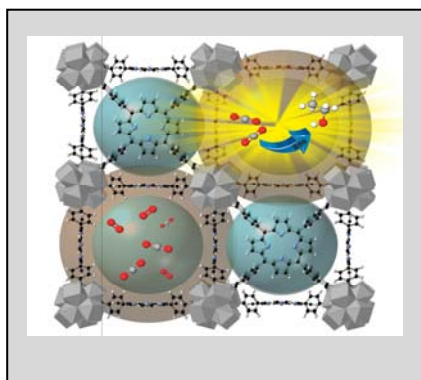
Keywords: artificial photosynthesis • CO₂ utilization • photochemistry • sustainable chemistry • reactive oxygen species

References:

- [1] H. Komiyama, S. Kraines, *Vision 2050: Roadmap for a Sustainable Earth*, Springer, Tokyo Berlin Heidelberg New York, 2008.
- [2] US Energy Information Administration Short-Term Energy Outlook (US Department of Energy, 2021).
- [3] J. Murray, D. King, *Nature* **2021**, *481*, 433.
- [4] IPCC Climate Change 2013: The Physical Science Basis (eds Stocker, T. F. et al.) (Cambridge Univ. Press, 2013).
- [5] J. Artz, T.E. Müller, K. Thenert, J. Kleinekorte, R. Meys, A. Sternberg, A. Bardow, W. Leitner, *Chem. Rev.* **2018**, *118*, 434.
- [6] Y. Tachibana, L. Vayssieres, J.R. Durrant, *Nat. Photonics* **2012**, *6*, 511.
- [7] J.Z. Zhang, E. Reisner, *Nat. Rev. Chem.* **2020**, *4*, 6.
- [8] P.K. Nayak, S. Mahesh, H.J. Snaith, D. Cahen, *Nat. Rev. Mater.* **2019**, *4*, 269.
- [9] J. Warnan, J. Willkomm, Y. Farre, Y. Pellegrin, M. Boujtita, F. Odobel, E. Reisner, *Chem. Sci.*, **2019**, *10*, 2758.
- [10] J. Waman, E. Reisner, *Angew. Chem. Int. Ed.* **2020**, *59*, 17344.
- [11] Y. Shiraishi, T. Takii, T. Hagi, S. Mori, Y. Kofuji, Y. Kitagawa, S. Tanaka, S. Ichikawa, T. Hirai, *Nat. Mater.* **2019**, *18*, 985.
- [12] S. Chen, T. Takata, K. Domen, *Nat. Rev. Mater.* **2017**, *2*, 1.
- [13] A. Fujishima, K. Honda, *Nature* **1972**, *238*, 37.
- [14] K.E. Dalle, J. Warnan, J. Leung, B. Reuillard, I.S. Karmel, E. Reisner, *Chem. Rev.* **2019**, *119*, 2752.
- [15] B. Zhang, L. Sun, *Chem. Soc. Rev.* **2019**, *48*, 2216.
- [16] F. Li, D.R. MacFarlane, J. Zhang, *Nanoscale* **2018**, *10*, 6235.
- [17] L.D. Ramírez-Valencia, E. Bailón-García, F. Carrasco-Marín, A.F. Pérez-Cadenas, *Catalysts* **2021**, *11*, 351.
- [18] W.-H. Wang, Y. Himeda, J.T. Muckerman, G.F. Manbeck, E. Fujita, *Chem. Rev.* **2015**, *115*, 12936.
- [19] Q. Liu, L. Wu, R. Jackstell, M. Beller, *Nat. Commun.* **2015**, *6*, 5933.
- [20] H. Rao, L.C. Schmidt, J. Bonin, M. Robert, *Nature* **2017**, *548*, 74.
- [21] Y. Wu, Z. Jiang, X. Lu, Y. Liang, H. Wang, *Nature* **2019**, *575*, 639.
- [22] J. Shen, R. Kortlever, R. Kas, Y.Y. Birdja, O. Diaz-Morales, Y. Kwon, I. Ledezma-Yanez, K.J.P. Schouten, G. Mul, M.T.M. Koper, *Nat. Commun.* **2015**, *6*, 8177.
- [23] I.I. Alkhatib, C. Garlisi, M. Pagliaro, K. Al-Ali, G. Palmisano, *Catal. Today* **2020**, *340*, 209.
- [24] R. Kuriki, M. Yamamoto, K. Higuchi, Y. Yamamoto, M. Akatsuka, D. Lu, S. Yagi, T. Yoshida, O. Ishitani, K. Maeda, *Angew. Chem. Int. Ed.* **2017**, *56*, 4867.
- [25] S. Lian, M.S. Kodaimati, D.S. Dolzhenkov, R., Calzada, E.A. Weiss, *J. Am. Chem. Soc.* **2017**, *139*, 8931.
- [26] C. Cometto, R. Kuriki, L. Chen, K. Maeda, T.-C. Lau, O. Ishitani, M. Robert, *J. Am. Chem. Soc.* **2018**, *140*, 7437.
- [27] Y. Pellegrin, F. Odobel, *C. R. Chimie* **2017**, *20*, 283.
- [28] H. Yuan, B. Cheng, J. Lei, L. Jiang, Z. Han, *Nat. Commun.* **2001**, *12*, 1835.
- [29] L. Duan, A. Fischer, Y. Xu, L. Sun, *J. Am. Chem. Soc.* **2009**, *131*, 10397.
- [30] R. Brimiouille, D. Lenhart, M.M. Maturi, T. Bach, *Angew. Chem. Int. Ed.* **2015**, *54*, 3872.
- [31] N.A. Romero, D.A. Nicewicz, *Chem. Rev.* **2016**, *116*, 10075.
- [32] E. Reisner, *Angew. Chem. Int. Ed.*, **2019**, *58*, 3656.
- [33] Q. Wang, J. Warnan, S. Rodríguez-Jiménez, J.J. Leung, S. Kalathil, V. Andrei, K. Domen, E. Reisner, *Nat. Energy* **2020**, *5*, 703.
- [34] M.F. Kuehnel, K.L. Orchard, K.E. Dalle, E. Reisner, *J. Am. Chem. Soc.* **2017**, *139*, 7217.
- [35] M. Jurow, A.E. Schuckman, J.D. Batteas, C.M. Drain, *Coord. Chem. Rev.* **2010**, *254*, 2297.
- [36] A.K. Burrell, M.R. Wasielewski, *J. Porph. Phthalocyanines* **2000**, *4*, 401.
- [37] J. Liu, Y. Li, S. Chen, Y. Lin, H. Lai, B. Chen, T. Chen, *Front Chem.* **2020**, *8*, 838.
- [38] S. Callaghan, M.O. Senge, *Photochem. Photobiol. Sci.* **2018**, *17*, 1490.
- [39] E.F.F. Silva, C. Serpa, J.P. Dabrowski, C.J.P. Monteiro, S.J. Formosinho, G. Stochel, K. Urbanska, S. Simoes, M.M. Pereira, L.G. Arnaut, *Chem. Eur. J.* **2010**, *16*, 9273.
- [40] I. Pibiri, S. Buscemi, A.P. Piccionello, A. Pace, *ChemPhotoChem*, **2018**, *2*, 535.
- [41] A.A. Ghogare, A. Greer, *Chem. Rev.* **2016**, *116*, 9994.
- [42] E.A. Dolgoplova, A.M. Rice, C.R. Martin, N.B. Shustova, *Chem. Soc. Rev.* **2018**, *47*, 4710.
- [43] M.D. Eisaman, K. Parajuly, A. Tuganov, C. Eldershaw, N. Chang, K.A. Littau, *Energy Environ. Sci.* **2012**, *5*, 7346.
- [44] J. Park, O. Jiang, D. Feng, L. Mao, H.-C. Zhou, *J. Am. Chem. Soc.* **2016**, *138*, 3518.
- [45] S. Freitag, B. Baumgartner, R. Radel, A. Schwaighofer, A. Varriale, A. Pennacchio, S. D'Auria, B. Lendl, *Lab Chip* **2021**, *21*, 1811.
- [46] S. Freitag, M. Baer, L. Buntzoll, G. Ramer, A. Schwaighofer, B. Schmauss, B. Lendl, *ACS Sens.* **2021**, *6*, 35.
- [47] J. Coates, Interpretation of Infrared Spectra: A Practical Approach. In: Meyers, R.A., Ed., *Encyclopedia of Analytical Chemistry*, John Wiley & Sons Ltd., Chichester, 10881-10882 (2000).
- [48] H. Fan, D. Wang, L. Wang, H. Li, P. Wang, T. Jiang, T. Xie, *Appl. Surf. Sci.* **2011**, *257*, 7758.
- [49] S. Schaden, M. Haberkorn, J. Frank, J.R. Baena, B. Lendl, *Appl. Spectrosc.* **2004**, *6*, 667.
- [50] J. Li, Y. Kuang, Y. Meng, X. Tian, W.-H. Hung, X. Zhang, A. Li, M. Xu, W. Zhou, C.-S. Ku, C.-Y. Chiang, G. Zhu, J. Guo, X. Sun, H. Dai, *J. Am. Chem. Soc.* **2020**, *142*, 7276.
- [51] Y.G. Li, J.C. Hao, H. Song, F.Y. Zhang, X.H. Bai, X.G. Meng, H.Y. Zhang, S.F. Wang, Y. Hu, J.H. Ye, *Nat. Commun.* **2019**, *10*, 2359.
- [52] J. Li, D. Luo, C. Yang, S. He, S. Chen, J. Lin, L. Zhu, X. Li, *J. Solid State Chem.* **2013**, *203*, 154.
- [53] Y. Zhang, K. Li, M. Chen, J. Wang, J. Liu, Y. Zhang, *ACS Appl. Nano Mater.* **2020**, *3*, 257.
- [54] X. Wu, Y. Li, G. Zhang, H. Chen, J. Li, K. Wang, Y. Pan, Y. Zhao, Y. Sun, Y. Xie, *J. Am. Chem. Soc.* **2019**, *141*, 5267.
- [55] Z.-B. Fang, T.-T. Liu, J. Liu, S. Jin, X.-P. Wu, X.-Q. Gong, K. Wang, Q. Yin, T.-F. Liu, R. Cao, H.-C. Zhou, *J. Am. Chem. Soc.* **2020**, *142*, 12515.
- [56] H.-Q. Xu, J. Hu, D. Wang, Z. Li, Q. Zhang, Y. Luo, S.-H. Yu, H.-L. Jiang, *J. Am. Chem. Soc.* **2015**, *137*, 13440.
- [57] H. Zhang, J. Wei, J. Dong, G. Liu, L. Shi, P. An, G. Zhao, J. Kong, X. Wang, X. Meng, J. Zhang, J. Ye, *Angew. Chem. Int. Ed.* **2016**, *55*, 14310.
- [58] Y. Liu, Y. Yang, Q. Sun, Z. Wang, B. Huang, Y. Dai, X. Qin, X. Zhang, *ACS Appl. Mater. Interfaces* **2013**, *5*, 7654.
- [59] N. Sadeghi, S. Sharifnia, M. Sheikh Arabi, *J. CO2 Util.* **2016**, *6*, 450.

-
- [60] S. Zhong, X. Yang, Z. Cao, X. Dong, S.M. Kozlov, L. Falivene, J.-K. Huang, X. Zhou, M.N. Hedhili, Z. Lai, K.-W. Huang, Y. Han, L. Cavallo, L.-J. Li, *Chem. Commun.* **2018**, *54*, 1124.
- [61] A. Halilu, M. Hayyan, M.K. Aroua, R., Yusoff, H.F. Hizaddin, W.J. Basirun, *J. Environ. Chem. Eng.* **2021**, *9*, 105285.
- [62] A. Halilu, M. Hayyan, M.K. Aroua, R. Yusoff, H.F. Hizaddin, *Phys. Chem. Chem. Phys.* **2021**, *23*, 1114.
- [63] R. Hanna, A. Abdulla, Y. Xu, D.G. Victor, *Nat. Commun.* **2021**, *12*, 368.
- [64] G. Realmonte, L. Drouet, A. Gambhir, J. Glynn, A. Hawkes, A.C. Köberle, M. Tavoni, *Nat. Commun.* **2019**, *10*, 3277.

Entry for the Table of Contents



A new approach to activate and convert CO₂ in dissolved as well as gaseous form via reactive oxygen species was established. Within only 5 h reaction time at atmospheric conditions, room temperature and without sacrificial donors a conversion efficiency of 92% from CO₂ to 12.2 mmol/L ethanol was achieved. Direct Air Capture experiments gave similar results, which showcases both the inherent flexibility of this method as well as its efficiency.

Supporting Information

Direct CO₂ Activation and Conversion to Ethanol via Reactive Oxygen Species

Alina Meindl^{[a],*} Senge M.O.,^[b,c]

Abstract: The growing demand for energy and the excessive use of fossil fuels represents one of the main challenges for humanity. Storing solar energy in the form of chemical bonds to generate solar fuels or value-added chemicals without creating additional environmental burdens is a key requirement for a sustainable future. Here we use biomimetic artificial photosynthesis and present a dPCN-224(H) MOF-based photocatalytic system, which uses reactive oxygen species (ROS) to activate and convert CO₂ to ethanol under atmospheric conditions, at room temperature and in 2-5 h reaction time without the use of sacrificial donors. The system provides a CO₂-to-ethanol conversion efficiency (CTE) of 92%, while attaining a selectivity for EtOH formation. Furthermore, this method also allows the conversion of CO₂ through direct air capture (DAC), making it an incredibly fast and versatile method for both dissolved and gaseous CO₂.

Table of Contents

Experimental Procedures	2
Results and Discussion	3
1. Linear Regression for Determination of CO ₂ Concentration	3
2. Spectra Exclusion Experiments	4
3. Reproducibility Experiments.	9
4. pH and DO Measurements	9
5. NMR-Spectra	11
6. Characterization Photocatalyst	12
References	13
Author Contribution	13

Experimental Procedures

Methods

General Materials

Unless otherwise specified, all chemicals were purchased from Sigma-Aldrich and used without further purification. 5,10,15,20-tetrakis(4-carboxyphenyl)porphyrin (CAS: 14609-54-2) was purchased from PorphyChem and used without further purification. The reactions were carried out in 5 mL transparent tamper evident sample tubes purchased from Sigma Aldrich (Z679038).

Photoactive material

dPCN-224(H)^[1]: As photosensitizer the nanomaterial dPCN-224(H) was used. The synthesis was performed according to a literature procedure and analytical data were in correspondence to those described in literature.

Photoinactive material/Blank material.

UiO-66 was used as the photo-inactive nanomaterial without a photosensitizer.^[2] Its synthesis was performed according to literature procedure.

Photochemical Experiments:

Photosynthetic reactions were carried out in a closed plastic container with side illumination from Paulmann MaxLED Tunable White 70623 with 870 lm luminous flux. 16 mg of photoactive material dPCN-224(H) were used per mL reaction media for all experiments. Samples for the ATR-measurements were taken at several points in time and injected into the flow cell. The reactions were performed at room temperature and under atmospheric conditions and no stirring was undertaken.

The CO₂ solutions were prepared by saturating cold distilled water (16-17 °C) with CO₂ gas in a closed system under pressure. The saturated CO₂ water was then diluted with distilled water (1:1; v/v) resulting in 4-4.2 ppm of dissolved O₂. The photoactive material was degassed in distilled water in the dark overnight. The catalyst was then put into 5 mL transparent tamper evident sample tubes prior to the addition of water, they were sealed and exposed to irradiation. The O₂ free solution was prepared by saturating distilled water with N₂ and then adding CO₂ gas. The ¹³CO₂ solutions were prepared by saturating distilled water with ¹³CO₂ gas. The gas was fed into a wash bottles containing distilled water. The wash bottles were placed in a temperature-controlled water bath at 20 °C. In order to perform the exclusion experiments without light the sample tubes were wrapped with tinfoil and kept in the dark to avoid any exposure to light. In order to perform the exclusion experiments without CO₂ only distilled water was added to the reaction. In order to perform the exclusion experiments without O₂ distilled water was degassed with N₂ for 2h before the CO₂ was added. The dissolved O₂ was measured with an oxygen sensor from Voltcraft to ensure the absence of O₂ (limit of detection 0.1 ppm). Furthermore, the container was purged with N₂ prior to the addition of the photoactive material and water and a protective N₂ layer was also added after the addition of the photosensitizer and water. In order to perform the exclusion experiments with the blank material UiO-66 was used instead of the photoactive material PCN-224.

Instrumentation

IR measurements:

IR measurements were performed with a previously published set-up.⁽³⁾

The experimental setup includes a multi-bounce ATR setup, linked to a US driver and a sequential injection analysis (SIA) system. The beam of a Vertex 70v (Bruker Optics, Ettlingen, Germany) FTIR spectrometer was guided through a custom-built ATR setup. The ATR fixture was 3D-printed using a Prusa Research i3 MK3 (Prague, Czech Republic) following blueprints constructed using Autodesk Inventor 2017 (Mill Valley, California, United States). The multi-bounce zinc sulphide (ZnS) ATR element (17 × 10 × 1 mm, 45°) was sourced from Crystran (Poole, United Kingdom). The flow cell geometry allowed for five accessible total reflections. The calculated effective thickness (de) achieved with the ATR element is 17.25 μm. The TE control was set to 37 °C throughout all assay experiments.

SUPPORTING INFORMATION

Prior to spectrum acquisition, the spectrometer was evacuated and the sample compartment was flushed with dry air. A spectral resolution of 4 cm^{-1} was set for recording spectra in double-sided acquisition mode. Each spectrum was an average of 128 scans (acquisition time: 16.9 s), calculated using a three-term Blackman–Harris apodization function and a zero-filling factor of 2. The aperture was set to 8 mm for maximum intensity throughput. The FTIR spectrometer was equipped with a liquid-nitrogen-cooled mercury cadmium telluride (HgCdTe) detector. Spectra were analyzed using the software package OPUS 8.2 (Bruker Optics, Ettlingen, Germany).

NMR measurements: ^1H -NMR spectra were recorded on a Bruker AVANCE-400 spectrometer.

UV/Vis spectroscopy: UV/Vis spectra were recorded on a Cary 50 Bio UV/Vis spectrophotometer (*Agilent Technologies*, USA) in quartz cuvettes with $d = 1\text{ cm}$ filled with 1.5 mL analyte solution between 200 - 800 nm.

Results and Discussion

1. Linear Regression for Determination of CO_2 Concentration

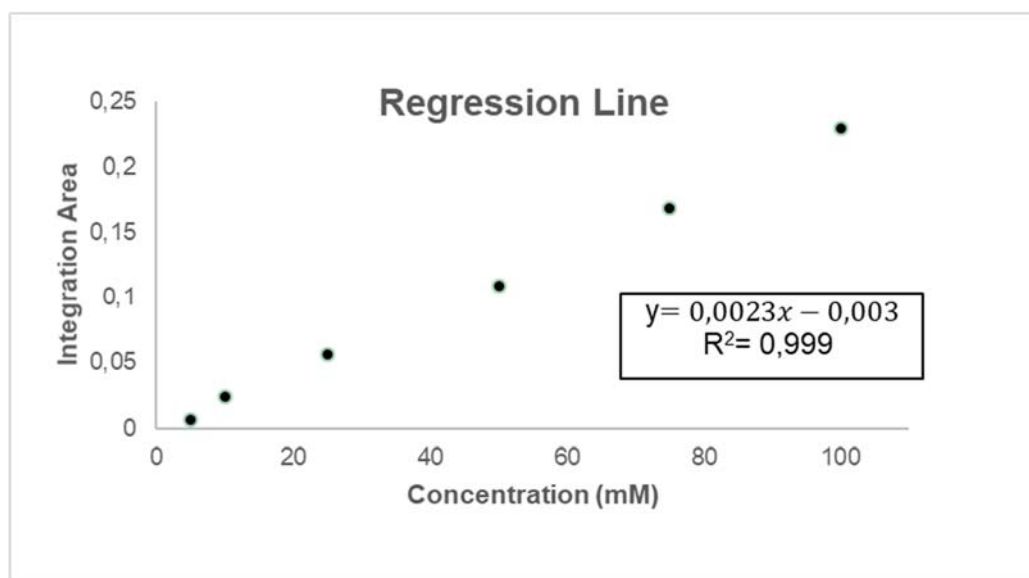


Figure S1: Linear Regression to calculate ETOH concentration.

2. Spectra Exclusion Experiments

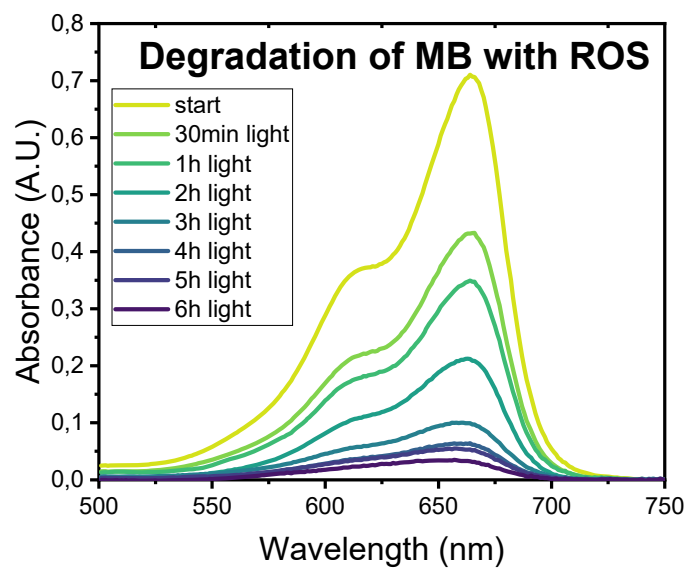


Figure S2: Degradation of Methylene blue by reactive oxygen species produced by the photosensitizer.

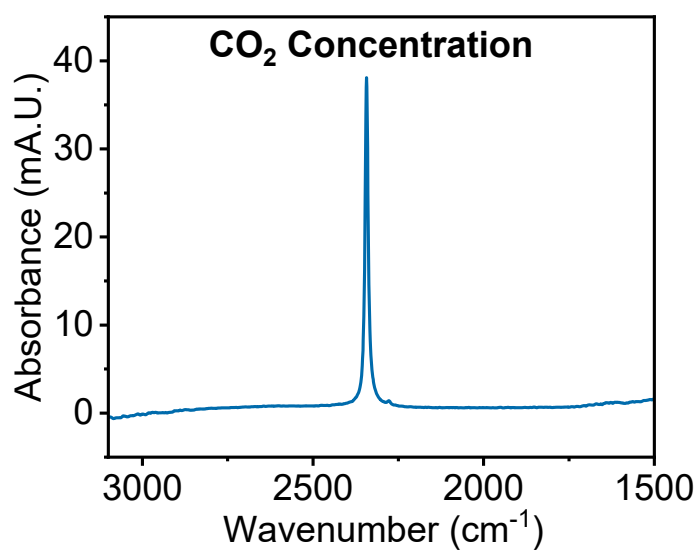


Figure S3: CO₂ concentration at the start of the reaction. Spectra was corrected for atmospheric CO₂ and distilled H₂O was used as background.

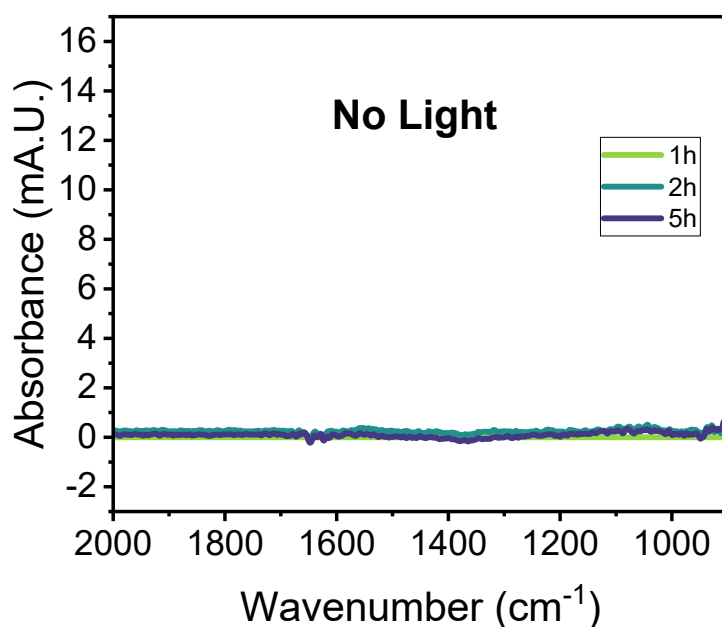


Figure S4: Exclusion experiment without light irradiation: no reaction. 100 mg catalyst were added to 6 mL distilled water/ CO₂ water (v/v =1:1) and kept in the dark. Background of the spectrum: distilled water.

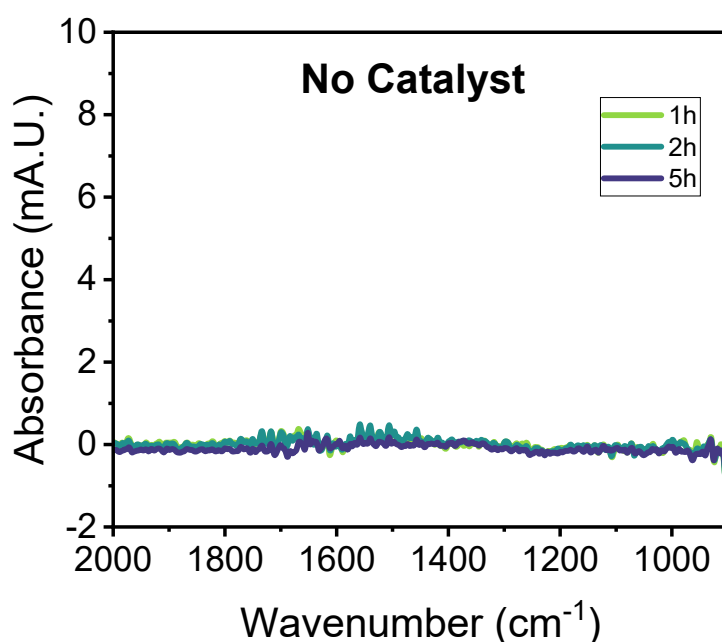


Figure S5: Exclusion experiment without photocatalyst: no reaction. 5 mL distilled water/ CO₂ water (v/v =1:1) was irradiated. Background of the spectrum: distilled water.

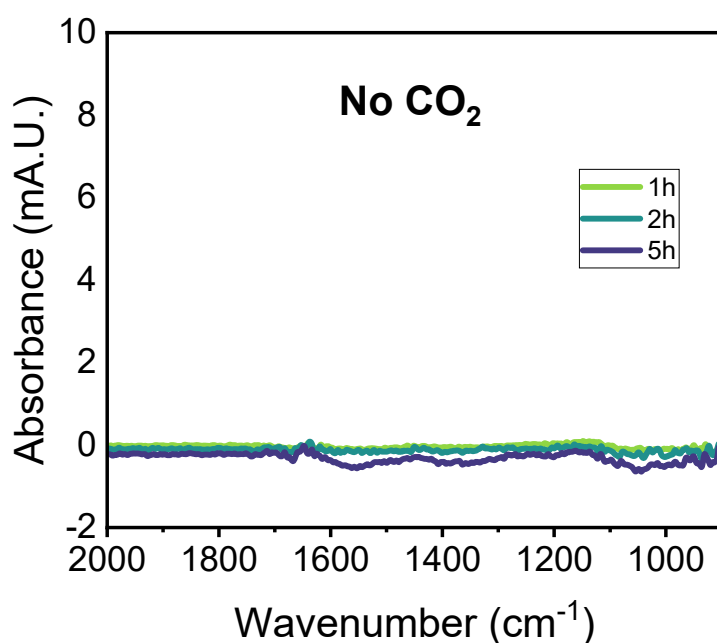


Figure S6: Exclusion experiment without CO₂: no reaction. 100 mg catalyst were added to 6 mL distilled water and irradiated. Background of the spectrum: distilled water.

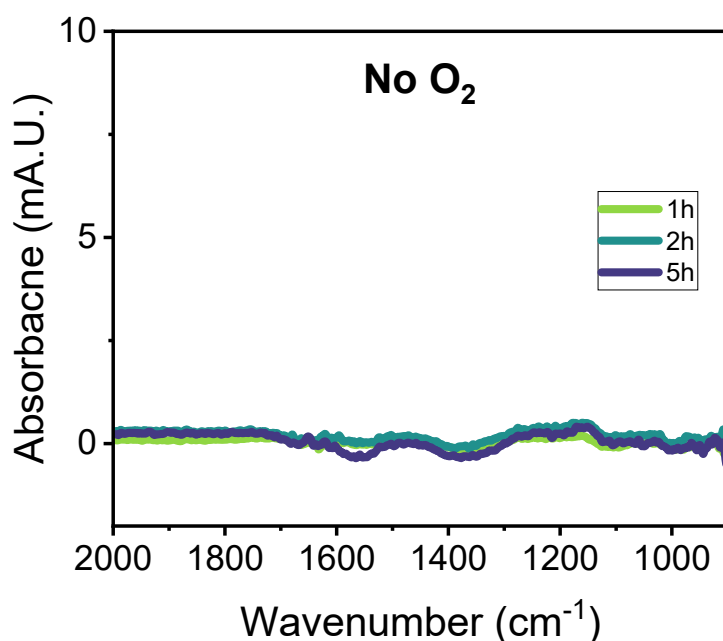


Figure S7: Exclusion experiment without O₂: no reaction. 140 mg catalyst were added to 8.9 mL distilled water (degassed with N₂ for 2h)/CO₂ water (v/v =1:1) and irradiated. Background of the spectrum: distilled water.

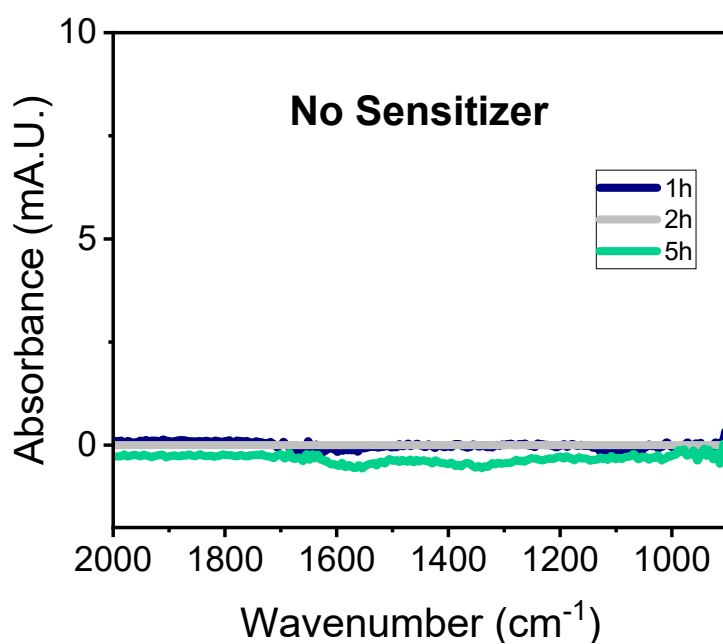


Figure S8: Exclusion experiment without photosensitizer: no reaction. 38 mg blank catalyst were added to 2.4 mL distilled water/ CO₂ water (v/v =1:1) and irradiated. Background of the spectrum: distilled water.

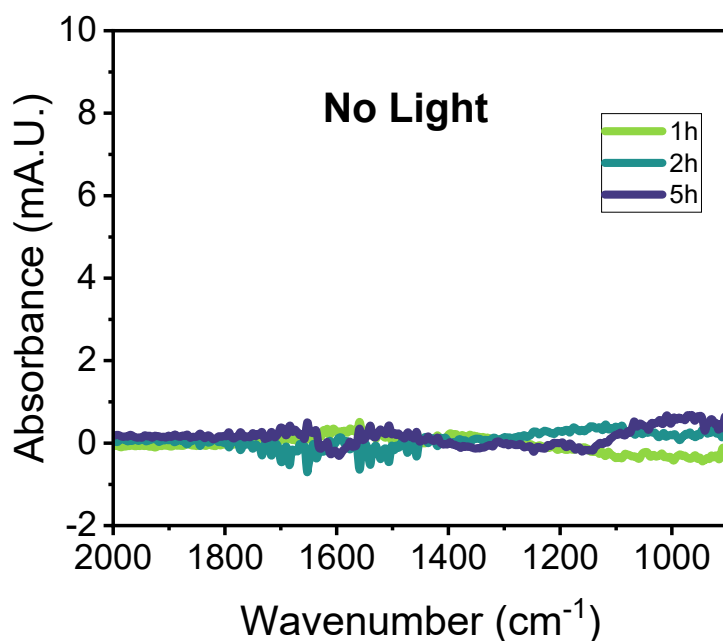


Figure S9: Exclusion experiments DAC without light: no reaction. 60 mg blank catalyst were added to 5mL distilled water and kept in the dark. Background of the spectrum: distilled water.

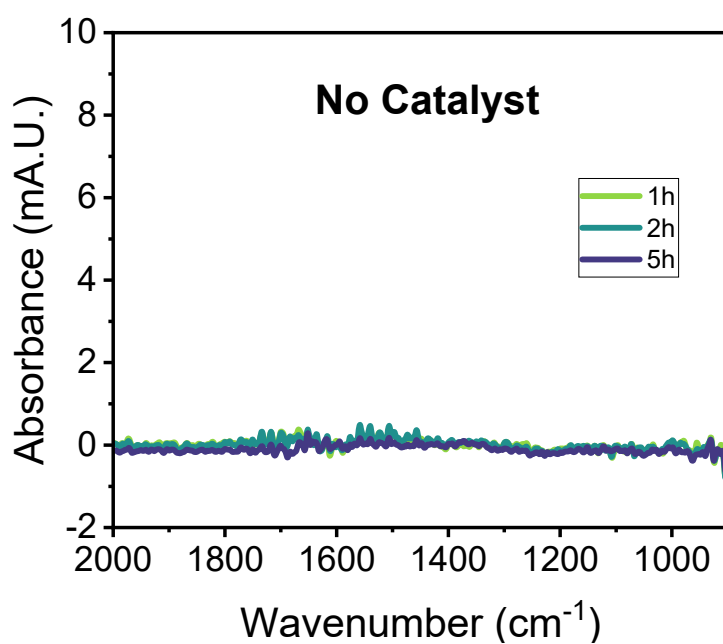


Figure S10: Exclusion experiment DAC without photocatalyst: no reaction. 5 mL distilled water were irradiated. Background of the spectrum: distilled water.

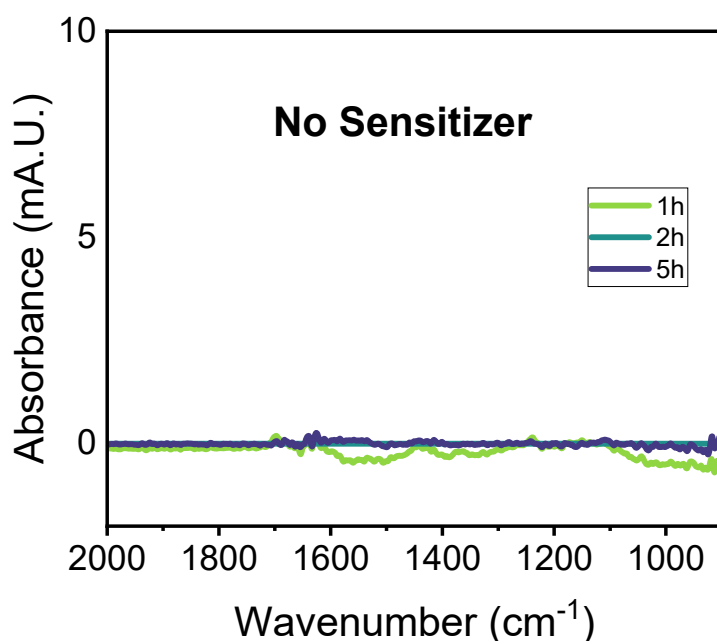


Figure S11: Exclusion experiment DAC without sensitizer: no reaction. 38 mg blank catalyst were added to 2.4 mL distilled water and irradiated. Background of the spectrum: distilled water.

SUPPORTING INFORMATION

3. Reproducibility Experiments.

Table S1: Reproducibility experiments.

Date	Concentration (mM) ^[a]	Concentration (Mol/L)
16.11.2020	9.86	0.0099
23.12.2020	12.47	0.0125
13.01.2021	9.86	0.0099
19.01.2021	10.38	0.0104
29.01.2021	11.43	0.0114
22.03.2021	10.38	0.0104

[a] Average: 10.73 mM; standard deviation: 0.94

4. pH and DO Measurements.

Table S2: pH and DO measurements during experiments.

Sample	pH	Temp (°C)	DO (ppm)
<u>Reaction CO₂</u>			
start	4.2	22.6	2.7
1h	4.4	22.3	3.7
2h	4.2	22.5	4
5h	4	22.6	4.1
24h	4.1	22.6	4.2
<u>Exclusion Experiment: No light</u>			
start	4.1	22.2	2.3
1h	4.2	22.7	3.2
2h	4.3	22.3	3.7
5h	4.5	22.6	4.2
<u>Exclusion Experiment: No catalyst</u>			
start	4	22.3	2.7
1h	4.2	22.5	3.7
2h	4.4	22.3	4
5h	4.4	22.6	4.4
<u>Exclusion Experiment: No CO₂</u>			
start	5.9	22.7	4.4
1h	5.7	22.5	4.9
2h	5.8	23	4.3
5h	5.4	22.7	4.6
<u>Exclusion Experiment: No O₂</u>			
start	4.2	22.5	0.1

SUPPORTING INFORMATION

1h	3.9	22.4	1.1
2h	4.3	22.7	1.6
5h	4.4	22.5	2.5

Exclusion Experiment: No sensitizer

blank start	4	22.3	2.7
blank 1h	4.6	22.6	2.4
blank 2h	4.4	23.1	3.4
blank 5h	4.4	23.1	4.5

Experiment: $^{13}\text{CO}_2$

start	4.5	22.5	4.1
1h	4.6	22.7	4.1
2h	4.2	22.8	4.1
5h	4.7	22.5	4.3
24h	4.2	22.7	4.5

Experiment: DAC

start	5.3	22.8	4.3
1h	5.1	22.5	4.2
2h	5.2	22.9	4.2
5h	5.4	22.6	4.7

Exclusion Experiment DAC: No light

start	5.4	22.6	4.4
1h	5.3	22.7	4.3
2h	5.2	22.5	4.2
5h	5.4	22.7	4

Exclusion Experiment DAC: No catalyst

start	5.4	22.7	4.3
1h	5.1	22.7	4.1
2h	5.2	22.5	4
5h	5.2	22.7	4.1

SUPPORTING INFORMATION

5. NMR-Spectra

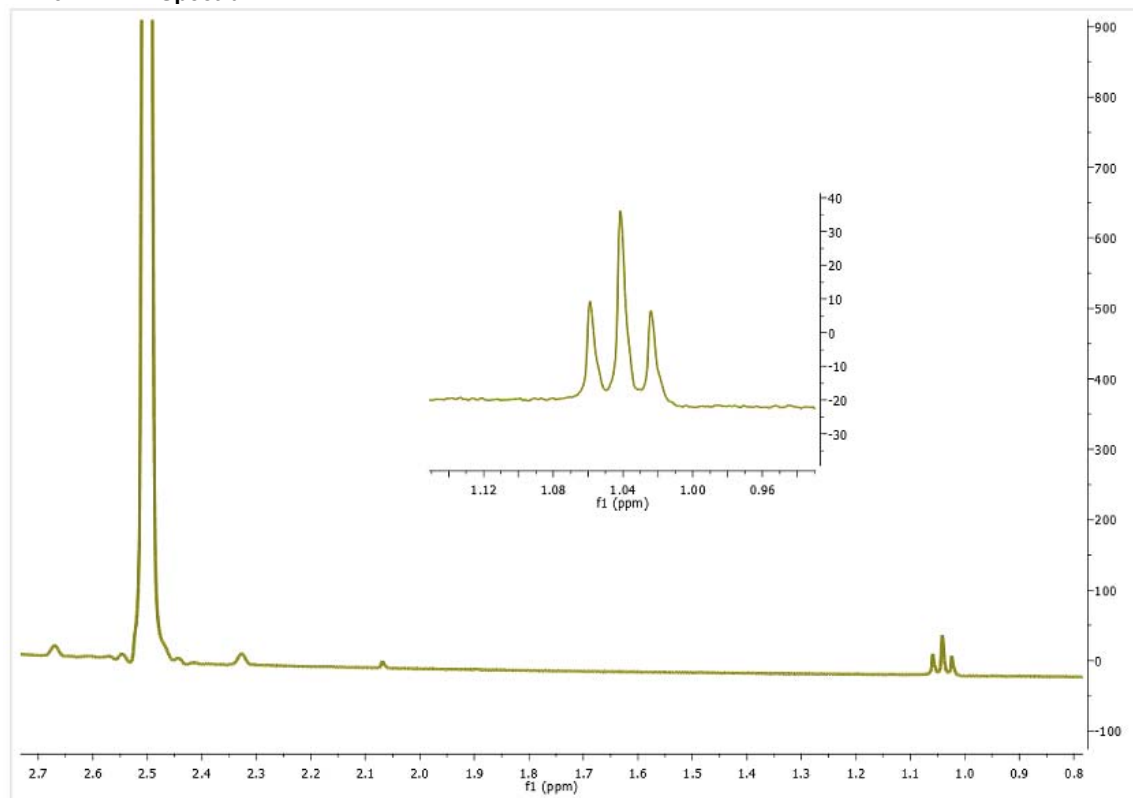
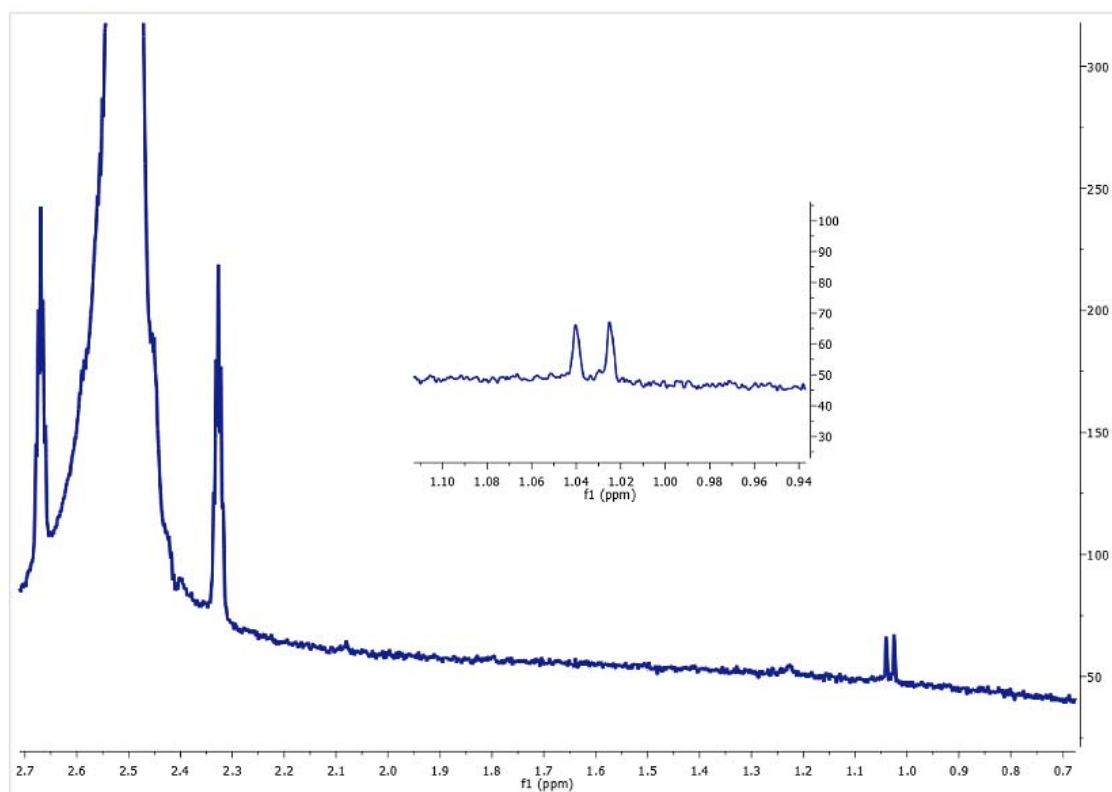


Figure S12: ¹H-NMR spectrum of EtOH from the photochemical reaction in DMSO.



SUPPORTING INFORMATION

Figure S13: $^1\text{H-NMR}$ spectrum of 2- ^{13}C -EtOH from the photochemical reaction in DMSO.

6. Characterization Photocatalyst

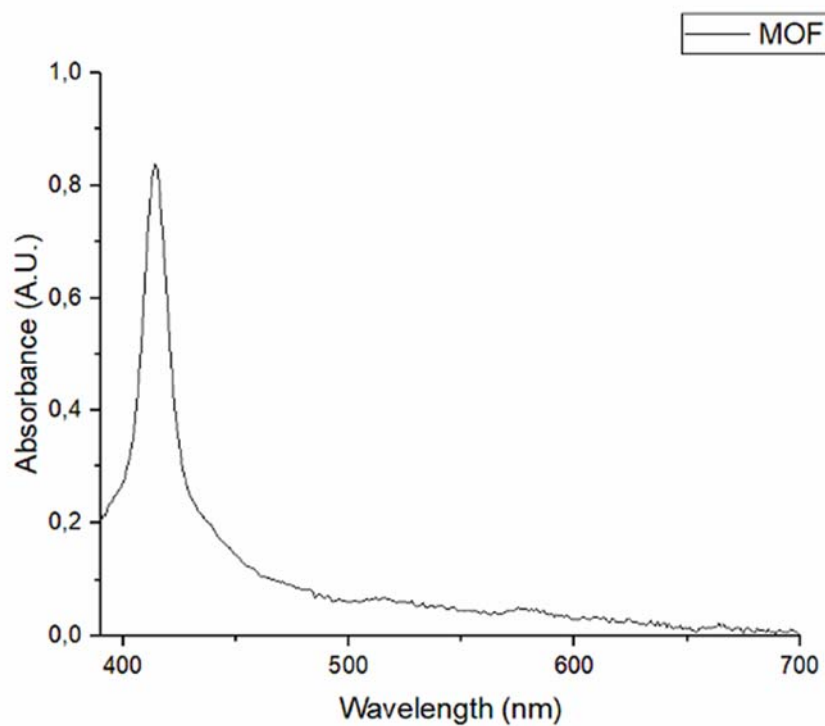


Figure S14.: UV/vis spectrum of PCN-224 photocatalyst in water.

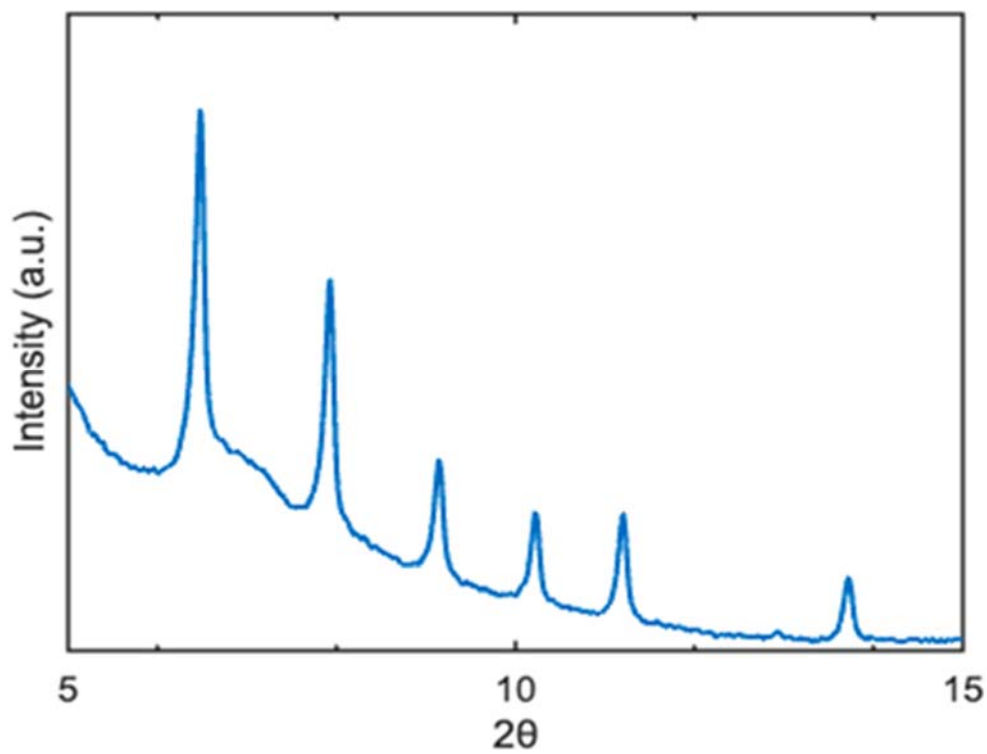


Figure S15: XRD of PCN-224 photocatalyst.

References

- [1] J. Park, Q. Jiang, D. Feng, L. Mao, H.-C. Zhou, *J. Am. Chem. Soc.* **2016**, *138*, 3518.
- [2] K.A. Kovalenko, V.P. Fedin, A.K. Sagidullin, B.M. Orliogdo, V.A. Bolotov, A.S. Knyazev, I.N. Mazov, S.L. Gorbin, V.S. Mal'kov, Patent of RF N°RU2719597C1 vol. 12, Bul. (2020).
- [3] S. Freitag, B. Baumgartner, S. Radel, A. Schwaighofer, A. Varriale, A. Pennacchio, S. D'Auria, B. Lendl, *Lab Chip*, **2021**, *21*, 1811.

Author Contributions

A.M.: project idea; conceptualization; designed and performed the experiments; formal analysis; writing: original draft; M.O.S.: contributed advice; funding acquisition; writing: review and editing;